Author contributions

Ge Yongkai: Conceptualization, Methodology, Software, Formal analysis, Investigation, Writing - Original Draft, Visualization.

Ma Yue: Conceptualization, Methodology, Software, Investigation, Writing - Original Draft.

Wang Qingrui: Conceptualization, Writing-review & editing.

Yang Qing: Resources, Conceptualization, Writing-review & editing, Data Curation, Supervision.

Lu Xing: Conceptualization, Writing-review & editing, Data Curation, Supervision.

Ba Shusong: Conceptualization, Writing-review & editing, Supervision.

Techno-economic-environmental assessment and performance comparison of a building distributed multi-energy system under various operation strategies

Yongkai Ge[a, b, #], Yue Ma[b, #], Qingrui Wang[b], Qing Yang[a,b,c,*], Lu Xing[d,*], Shusong Ba[e,*]

[a]China-EU Institute for Clean and Renewable Energy, Huazhong University of Science and Technology, Wuhan, 430074, PR China

[b]State Key Laboratory of Coal Combustion, Huazhong University of Science and Technology, Wuhan, 430074, PR China

[c]John A. Paulson School of Engineering and Applied Sciences, Harvard University, Cambridge, MA, 02138, USA

[d]Mechanical and Construction Engineering, Northumbria University, Newcastle upon Tyne, NE1 8ST, United Kingdom

[e]Peking University HSBC Business School, Peking University, Shenzhen, 518055, PR China

*Corresponding author:

Qing Yang, qyang@hust.edu.cn

Lu Xing, lu.xing@northumbria.ac.uk

Ba Shusong, bashusong@163.com

# The author contributed equally to this work

Abstract

The distributed energy system (DES) is a promising technology that could enable decarbonization in the building sector. Comprehensive DES system assessment from a holistic perspective is crucial for system design, operation strategy selection, and performance optimization. This paper proposes a techno-economic-environmental integrated assessment model for comprehensive system evaluation. The DES configuration mainly includes a photovoltaic panel, ground source heat pump, gas turbine, absorption heat pump, and thermal storage tank. The system is simulated under three operation strategies with MATLAB/Simulink, which are following thermal load (FTL), following electric load (FEL), and following electric load with thermal storage (FELTS). Entropy-TOPSIS method is used to evaluate the DES's techno-economic-environmental performance under various operation strategies. The results indicate that the DES' primary energy efficiency ratio under the three operation strategies of FTL, FEL and FELTS are 51.49%, 86.78%, and 125.69%, respectively. The dynamic annual values are 1.05×10^6 CNY, 7.23×10^5 CNY, and 5.94×10^5 CNY, respectively. The total greenhouse gas emissions are 36.2 kg CO2eq/$(m^2 \cdot a)$, 22.8 kg CO2eq/$(m^2 \cdot a)$, and 16.4 kg CO2eq/$(m^2 \cdot a)$, respectively. The entropy-TOPSIS analysis results showed that under FELTS operation strategy, DES performs the best; it has the best indicators for technical and environmental evaluation.

Keywords: Distributed energy system; Energy storage; Life cycle assessment; Operation strategy; Entropy weight method; Technique for order preference by

similarity to an ideal solution

1. Introduction

Buildings accounted for 36 percent of global energy demand and 37 percent of energy-related carbon dioxide emissions in 2020 [1]. To develop a sustainable and low-carbon society, energy conservation and emission reduction in the building sector play an increasingly significant role [2]. In China, building electricity, heating, and cooling demands are mainly satisfied by fossil-fueled thermal power plants and air conditioners with relatively low energy efficiency [3-5], and it causes a severe pollution problem. To mitigate environmental impact while meeting the increasing building energy demand, many scholars worldwide focus efforts on the research of DES [6].

The DES combines renewable energy utilization devices and the combined cooling, heating, and power (CCHP) system to supply buildings with electricity, heating, and cooling energy [7-9]. Renewable energy is rich in resources and pollution-free, and the CCHP system realizes cascade utilization of energy [10-13]. This system integration improves total system efficiency and reduces emissions [14]. The integrated DES can provide varying thermal and electric energy to meet the actual building energy demand [15, 16]. The building demands vary throughout the year, and the inappropriate control strategy causes energy shortages or energy waste problems. Research on system modeling, operation strategy, and comprehensive performance evaluation is critical for developing and applying the DES.

Some scholars focus on optimizing DES equipment configuration and capacity. Chen et al. analyzed the application of gas-fired CCHP and Ground source heat pump (GSHP) coupling systems in a commercial park. The results showed that the coupling system consumes less energy and demonstrates less environmental impact than the conventional system [17]. Boyaghchi et al. established a new model of a micro CCHP system powered by solar and geothermal energy. The non-dominated sorting genetic algorithm II was used to perform the multi-objective system optimization [18]. Lombardo et al. developed a solar-driven CCHP system and tested its performance. The system operates on average about 2400 hours per year, while the system efficiency in different regions can reach 32% to 42% [19]. Wang et al. derived a thermodynamic analysis for a CCHP system bases on solar thermal biomass gasification [20]. Mehrpooya et al. investigated the performance of CCHP system coupling with solid oxide fuel cells and performed a case study in Tehran [21].

The studies mentioned above compared different types of energy systems' performance or optimized system performance under one specific operation strategy. A comparison of the DES system performance under different operation strategies is needed. Zhang et al. compared the energy, economic and environmental performance of CCHP systems under various operation strategies: following hybrid electric-thermal load, following thermal load, and following electric load [22]. Results showed that the system performed the best under FEL. Ren et al. found that the DES performance under FTL and FEL is better than the traditional centralized energy supply system [23]. Zhu et al. studied the optimal combination, capacity, and operation strategy of the CCHP system with renewable energy. The net present value, internal rate of return, and dynamic payback period are used as economic indicators, and the carbon dioxide emission reduction rate is used as environmental protection indicator [24]. Ren et al. optimized and compared the performance of a DES under different operation strategies, and the results showed that the FEL has the best performance [25]. Das et al. established a hybrid energy system integrating two prime movers (internal combustion engine and micro gas turbine) and photovoltaic (PV) modules under various operation strategies. Results showed that the system demonstrates higher overall efficiency and better environmental performance under the FEL operation strategy [26]. Brandoni et al. conducted a study to optimize DES performance. The integrated DES includes micro CCHP and the high-concentration photovoltaic power generation system [27]. The multi-objective optimization of DES system performance under different operation strategies, such as FEL, FTL, etc., has been studied [28].

Some research work utilized the life cycle assessment (LCA) method for evaluating the system's environmental impact, but most of the researches didn't consider the environmental impact in the multi-objective optimization process presented above. Yang et al. used LCA and analyzed the optimal capacity of a CCHP system with biomass gasification. Results showed that the system's techno-Economic-Environment performance indicators increased first and then decreased with system capacity increase, and the optimal capacity is 5 MW [29]. Jing et al. studied the building cogeneration system's primary energy consumption and pollutant emission under the FEL and FTL through LCA [30]. Peppas et al. developed a zero-carbon emission renewable energy-hydrogen hybrid energy system with LCA. Compared with the municipal grid hybrid power system, the system's global warming potential, acidification potential, and photochemical oxidant generation are reduced by 40%, 42%, and 35%, respectively [31].

Researchers investigated the DES's configuration and capacity optimization, operation strategy optimization, LCA, and system comprehensive evaluation. Although existing research emphasizes the importance of optimization and evaluations for distributed energy systems for their development and applications, most studies focus on evaluations from techno-economic aspects or for a relatively short operational time. Li et al. used the Technique for Order Preference by Similarity to an Ideal Solution (TOPSIS) to optimize the biomass gasification-based CCHP system for a hypothetical hotel building in six different climate zones in China [32]. Wang et al. developed a quantitative multi-criteria methodology for building retrofitting programs by integrating the benefits of variable clustering and TOPSIS [33].

There is a lack of research on the DES performance under different operation strategies over a long operational time and, most importantly, evaluation and comparison of the system performance under different operation strategies from a holistic perspective. Thus, research on the evaluation of DES systems' performance from a holistic perspective should be performed; this includes proposing a normalized evaluation process and comparing the performance of DES under various operation strategies using the proposed evaluation process.

This paper presented a techno-economic-environmental integrated assessment model for the DES system. The DES utilizes the PV, GSHP, gas turbine (GT), absorption heat pump (AHP), and thermal storage tank (TST) to meet building electricity, heating, and cooling demands. The system simulation method uses MATLAB software to simulate the system operation status and techno-economic evaluation, while the LCA method is used for environmental evaluation. The Entropy-TOPSIS method is proposed for the techno-economic-environmental integrated systematic performance evaluation. We proposed a novel operation strategy FELTS for the DES. The holistic system analysis results of the DES system under the FELTS are compared to system results under the two conventional operation strategies, which include FTL and FEL, and the results are discussed.

2. Methodology and Case Analysis

2.1. Distributed Energy System

The DES consists of PV, GT, GHSP, AHP, TST, and auxiliary equipment. The system is powered by solar energy, natural gas, geothermal energy, and electric energy to meet the corresponding cooling, heating, and power energy demand for the building.

2.1.1. Photovoltaics model

The power generation and efficiency mainly depend on the PV panels' temperature and solar radiation intensity [34-36]. The surface temperature is affected by ambient temperature:

$$T_c = T_{\mathrm{ref}} + K \cdot G_{AC} \tag{1}$$

Where T_c is the realistic temperature of PV panel (K), T_{ref} is the ambient temperature (K), K is the temperature coefficient of PV panel and the value is 0.03, G_{AC} is the solar radiation intensity (W/m^2). The output power of PV module is determined by panel temperature and solar radiation intensity:

$$P_{PV} = P_{STC} \cdot [1 - 0.0047(T_c - T_r)] \cdot \frac{G_{AC}}{G_{STC}} \quad (2)$$

Where P_{PV} is the output power of the PV module (kW), P_{STC} is the maximum output power under standard test conditions (kW), T_r is the reference temperature of the PV module, and the value is 25℃, G_{STC} is the solar radiation intensity under standard test conditions, and the value is 1000 W/m^2.

2.1.2. Ground source heat pump model

The GSHP is a heating/cooling system for the building [37, 38], and the Gordon model is used for calculating heat pump output power [39]:

$$W = \frac{Q_e + q_e}{T_{ch,out}} \cdot T_{cl,in} - q_c + (f_{HX} - 1) \cdot Q_e \quad (3)$$

Where W is the heat pump output power (W), $T_{cl,in}/T_{ch,out}$ is the inlet/outlet cooling water temperature of condenser (K), q_c/q_e is the heat loss in condenser/evaporator (W), Q_e is the cooling load (W), f_{HX} is the coefficient reflecting various working conditions. Equation (4) is determined by the least-square fitting of Equation (3) using the manufacture-provided data:

$$\frac{W}{Q_R} = (L + 0.667) \cdot \frac{T_{cl,in}}{T_{ch,out}} - 1.001 \cdot L - 0.651 \quad (4)$$

Where Q_R is the heat pump rated power (kW), L is the heat pump partial load rate. In heating mode, the COP of the heat pump can be expressed as:

$$COP = \frac{Cap_{heating}}{P_{heating}} \tag{5}$$

Where $P_{heating}$ is the consumed heat pump power in heating mode (kW), $Cap_{heating}$ is the heat transferred by the heat pump (kW). The heating energy absorbed by the heat pump from the soil is:

$$Q_{absorbed} = Cap_{heating} - P_{heating} \tag{6}$$

The outlet water temperature at the source side and load side of the heat pump are shown as follows:

$$T_{source,out} = T_{source,in} - \frac{Q_{absorbed}}{m_{source} \cdot Cp_{source}} \tag{7}$$

$$T_{load,out} = T_{load,in} + \frac{Cap_{heating}}{m_{load} \cdot Cp_{load}} \tag{8}$$

Where $T_{source,in}$ / $T_{load,in}$ is the inlet water temperature of heat pump on the source/load side (K), Cp_{source}/Cp_{load} is the specific heat of circulating fluid on the source/load side (kJ/(kg · K)), m_{source}/m_{load} is the water flow on the source/load side (kg/s).

2.1.3. Gas turbine model

The natural gas turbine is a common choice for the prime mover of the CCHP system. The operating performance of the GT is mainly affected by system partial load rates and ambient temperature [40, 41]. Below presented the equations for the gas turbine model.

$$\begin{cases} P_{GT} = p_1(t)E_{GT} + q_1(t)\delta_{GT} \\ p_1(t) = a_1 t + b_1 \\ q_1(t) = c_1 t + d_1 \\ Q_{GT} = p_2(t)E_{GT} + q_2(t)\delta_{GT} \\ p_2(t) = a_2 t + b_2 \\ q_2(t) = c_2 t + d_2 \\ E_{GT\_\max} = E_{GT0\_\max}\left[1 - k_1(t-t_0)^3 - k_2(t-t_0)^2 - k_3(t-t_0) - k_4\right] \\ E_{GT\_\min}\delta_{GT} \le E_{GT} \le E_{GT\_\max}\delta_{GT} \end{cases} \tag{9}$$

Where E_{GT} is the fuel consumption of GT (kW), δ_{GT} is the binary state parameter of GT, Q_{GT} is the residual heating energy in the exhaust gas of GT (kW), t is the ambient temperature (°C), t_0 is the ambient temperature under the design condition, 15℃, $E_{GT,min}/E_{GT,max}$ is the fuel consumption of GT under the minimum/maximum load state (kW), p_1, p_2, q_1, q_2 are the parameters related to the ambient temperature. The remaining variables, a_i , b_i and c_i are coefficients to be determined. The performance curve of GT is fitted with manufacturer data. The output power of GT under different ambient temperatures is as follows:

$$P_m = \begin{cases} 107.5(t < 283.15K) \\ 0.005275t^2 - 1.437t + 121.1(t \ge 283.15K) \end{cases} \tag{10}$$

$$P_{GT} = plr \cdot P_m \tag{11}$$

Where P_m is the maximum output power of GT (kW). The power generation efficiency of GT at full load rate can be expressed as:

$$eff_m = \begin{cases} 0.3075(t < 283.15K) \\ -0.001063t^2 - 0.1134t + 31.98(t \ge 283.15K) \end{cases} \tag{12}$$

The power generation efficiency of GT should be re-calculated due to the influence of partial load rate:

$$eff = k_{eff} \cdot eff_m \tag{13}$$

$$k_{eff} = a_0 + \sum_{n=1}^{2} a_n \cdot cos(nwP_{GT}) + b_n \cdot sin(nwP_{GT}) \quad (14)$$

Where eff is the generation efficiency of GT, k_{eff} is the correction coefficient of GT efficiency, and the remaining parameters are constants. The fuel consumption of GT and heating energy of exhaust gas can be calculated as:

$$E_{GT} = \frac{P_{GT}}{eff} \quad (15)$$

$$Q_{GT} = E_{GT} \cdot (1 - eff) \quad (16)$$

2.1.4. Absorption heat pump model

The waste heating energy of the GT can power AHP. The afterburner (AB) ensures that the AHP has an adequate driving heat source. The performance curve of AHP is shown as follows:

$$COP_c = \frac{COP_{rc} \cdot plr_{ac}}{0.75plr_{ac}^2 + 0.0195plr_{ac} + 0.213} \quad (17)$$

$$COP_h = \frac{COP_{rh} \cdot plr_{ac}}{0.22plr_{ac}^2 + 0.6698plr_{ac} + 0.112} \quad (18)$$

$$\begin{cases} Q_{AC} = (Q_{GT} + Q_{AB}) \cdot COP_c \\ Q_{ACmin} \cdot \delta_{AC} \le Q_{AC} \le Q_{ACmax} \cdot \delta_{AC} \end{cases} \quad (19)$$

$$\begin{cases} Q_{AH} = (Q_{GT} + Q_{AB}) \cdot COP_h \\ Q_{AHmin} \cdot \delta_{AH} \le Q_{AH} \le Q_{AHmax} \cdot \delta_{AH} \end{cases} \quad (20)$$

Where COP_c and COP_h are the realistic cooling and heating efficiency, COP_{rc} and COP_{rh} are the nominal cooling and heating efficiency, plr_{ac} is the partial load rate, Q_{AC} and Q_{AH} are the cooling and heating capacity from flue gas (kW), δ_{AC} and δ_{AH} are cooling and heating binary state parameters, Q_{ACmin}/Q_{AHmin} is the minimum cooling/heating capacity (kW), Q_{ACmax}/Q_{AHmax} is the maximum cooling/heating capacity (kW), Q_{AB} is the heating energy provided by the AB (kW).

2.1.5. Thermal storage tank model

When the system cooling or heating energy supply exceeds the building energy demand, the TST is in the energy storage state. On the contrary, the TST is in the energy release state. The energy stored in the TST at the time *i* is shown as follows:

$$Q_{tst}^{i} = \eta_{tst} Q_{tst}^{i-1} + \alpha_{tst,in}^{i-1} Q_{tst,in}^{i-1} - \alpha_{tst,out}^{i-1} Q_{tst,out}^{i-1} \tag{21}$$

Where Q_{tst}^{i} is the energy stored in TST at time *i* (kW), Q_{tst}^{i-1} is the energy stored in TST at time *i*-1 (kW), $Q_{tst,out}^{i-1}$ is the output energy from TST at time *i*-1 (kW), η_{tst} is the heat storage efficiency of TST, $\alpha_{tst,in}^{i-1}$ and $\alpha_{tst,out}^{i-1}$ is the binary state parameter.

2.2. Operation Strategies

2.2.1. Following the thermal load

The system control logic of FTL is as follows: Building cooling and heating load determine the residual heat of gas required by the AHP, and the GT's power generation is then determined. The GSHP is turned on when the AHP cannot satisfy the building's cooling or heating load. The GT, PV, and grid supply power to meet the electric demand. Under the FTL strategy, the energy balance of the system can be expressed as follows：

$$E_{\mathrm{grid}} + P_{PV} + P_{GT} \geq E_{dem} + W_{GSHP} \tag{22}$$

$$Q_{h,AHP} + Q_{h,GSHP} = Q_{h,dem} \tag{23}$$

$$Q_{c,AHP} + Q_{c,GSHP} = Q_{c,dem} \tag{24}$$

Where E_{grid}, P_{PV} and P_{GT} are the power from the grid, PV and GT, respectively (kW), E_{dem} and W_{GSHP} are the power demand of the building and GSHP (kW), $Q_{h,AHP}$ and $Q_{c,AHP}$ are the heating and cooling energy supply of the AHP (kW), $Q_{h,GSHP}$ and $Q_{c,GSHP}$ are the heating and cooling energy supply of the GSHP (kW), $Q_{h,dem}$ and $Q_{c,dem}$ are the building heating and cooling loads (kW). The system's energy conversion and equipment configuration is shown in Fig. 1.

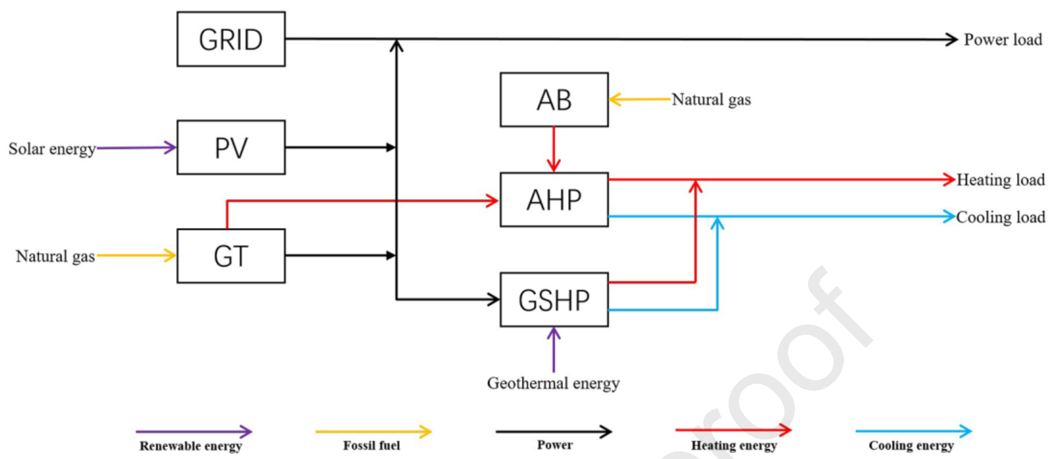

Fig. 1: The configuration of the DES under FTL.

2.2.2. Following the electric load

The system configuration under the FEL is the same as the system under the FTL. The system control logic of FEL is as follows: The electric load and the power generation of PV modules determine the GT power generation, and the cooling and heating capacity from the AHP under this power generation is then calculated. If the AHP provided cooling and heating can not meet the building demands, GSHP is used as supplementary energy to fill the gap. Under the FEL strategy, the energy balance of the system can be expressed as:

$$E_{grid} + P_{PV} + P_{GT} \geq E_{dem} + W_{GSHP} \quad (25)$$

$$Q_{h,AHP} + Q_{h,GSHP} \geq Q_{h,dem} \quad (26)$$

$$Q_{c,AHP} + Q_{c,GSHP} \geq Q_{c,dem} \quad (27)$$

2.2.3. Following the electric load with thermal storage

Under FTL or FEL operation strategies, the system produces an excessive energy supply. Thus, integrating energy storage devices into the system is necessary for eliminating energy waste, and the operation strategy of FEL integrated with TST (FELTS) is proposed. The system control logic under FELTS is almost the same as the FEL. For the FELTS, when there is a difference between energy demand and supply, the stored energy is used as a primary supplement. Under the FELTS strategy, the energy balance of the system can be expressed as follows:

$$E_{grid} + P_{PV} + P_{GT} \geq E_{dem} + W_{GSHP} \tag{28}$$

$$Q_{h,AHP} + Q_{h,GSHP} + Q_{h,TST} \geq Q_{h,dem} \tag{29}$$

$$Q_{c,AHP} + Q_{c,GSHP} + Q_{c,TST} \geq Q_{c,dem} \tag{30}$$

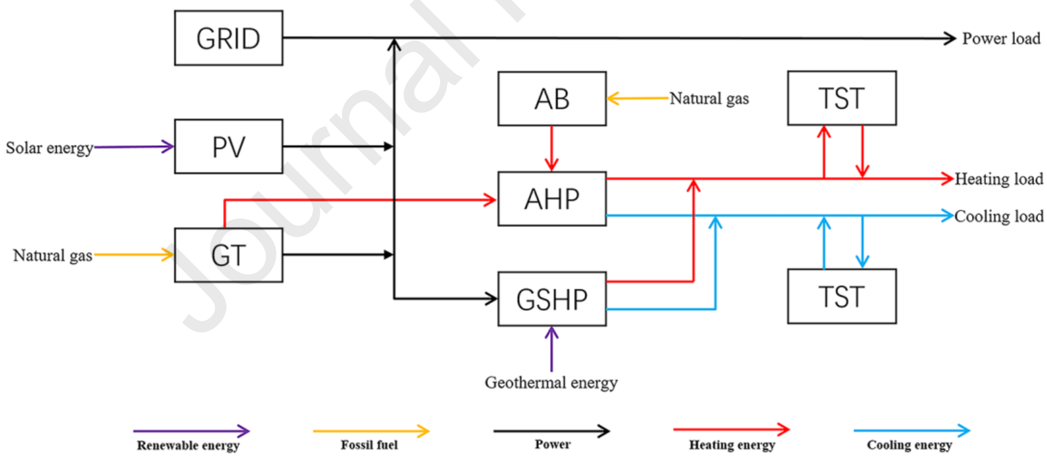

Fig. 2: The configuration of the DES under FELTS.

2.3. Techno-Economic-Environment Assessment

2.3.1. Energy evaluation index - PER

The non-renewable primary energy efficiency ratio (PER) is used as the energy evaluation index [42]. In this paper, the non-renewable primary energy consumption

(PEC) refers to the sum of the total natural gas consumed by the DES and the non-renewable primary energy consumed by the electricity purchased from the municipal power network:

$$Q_{DES} = Q_{GT} + Q_{AC} + \frac{E_{\text{grid}}}{\eta_p \eta_l} \tag{31}$$

Where Q_{DES} is the PEC of DES (kWh), Q_{GT} is the natural gas consumption of GT (kWh), Q_{AC} is the natural gas consumption of AHP (kWh), E_{grid} is the electricity purchased from the grid (kWh), η_p is the electricity generation efficiency of the grid and the value is 0.35, η_l is the transmission efficiency and the value is 0.93. PER is the ratio of the total building energy demand satisfied by the system to the total PEC and it reflects the effective energy utilization of the system, and the expression is:

$$PER = \frac{Q_e + Q_{cooling} + Q_{heating}}{Q_{DES}} \tag{32}$$

Where Q_e is the power load of the building (kWh), $Q_{cooling}$ is the cooling load of the building (kWh), $Q_{heating}$ is the building heating load (kWh).

2.3.2. Economic evaluation index - DAV

The dynamic annual-cost value (DAV) is selected as the economic evaluation index [43, 44]. DAV considers the influence of initial investment, annual operation cost, and maintenance cost:

$$DAV = C_c + C_{op} + C_m \tag{33}$$

$$C_c = \frac{i(1+i)^n}{(1+i)^n - 1} C_0 \tag{34}$$

Where C_c is the annual discounted cost of initial investment (CNY), C_0 is the initial investment of the system (CNY), C_{op} is the annual operation cost of the system (CNY),

C_m is the annual maintenance cost of the system (CNY), i is the interest and the value is 6%, n is the devices operational lifetime, 20 years. The initial investment of the system is composed of the purchase and installation costs. The purchase cost can be calculated as:

$$C_{p0} = \sum_{k=1}^{l} N_k C_k \tag{35}$$

Where C_{p0} is the purchase cost (CNY), N_k is the capacity of the k-th equipment (kW), C_k is the price of unit capacity (CNY/kW). The installation cost is calculated as a percentage of the equipment cost. The initial investment of the system can be calculated as:

$$C_0 = C_{\mathrm{p0}} + C_{i0} \tag{36}$$

Where C_{i0} is the system installation cost (CNY). The system annual operation cost is the sum of the energy consumption costs in a year, which includes the natural gas cost and the cost of purchasing power from the grid:

$$C_{\mathrm{op}} = BC_{gas} + E_{grid}C_e \tag{37}$$

Where B is the natural gas consumption of the system in the whole year (m^3), C_{gas} is the price of natural gas (CNY/m^3), C_e is the power price of the grid (CNY/kWh). The system annual maintenance cost is calculated by the proportional coefficient method:

$$C_m = \varepsilon C_c \tag{38}$$

Where ε is the maintenance cost coefficient, and the value is 0.03.

2.3.3. Environment evaluation index - LCA

LCA is a common method for the quantitative evaluations of system environmental impact [45-47]. According to the ISO international standard, LCA has four main phases: goal and scope definition, inventory analysis, impact assessment, and interpretation.

Goal and scope definition. This paper evaluates the DES system's full-lifecycle environment impact to identify the optimal operation strategies and improve the system efficiency. Through LCA evaluations, it assesses and compares the DES system's environmental impact under three operation strategies.

System boundary and function unit. The reference service life of various subsystems is set to 20 years. This paper implements the “cradle-to-grave” research process. The life cycle is analyzed from four phases: raw material acquisition and manufacturing stage (AM), transportation and installation stage (TI), operation and maintenance stage (OM), scrapping and disposal stage (SD). The system boundary of DES is displayed in Fig. 3. To represent and compare the environmental impact of DES under various operation strategies, the function unit is used in the LCA method. The defined function unit is one square meter of flooring during one year.

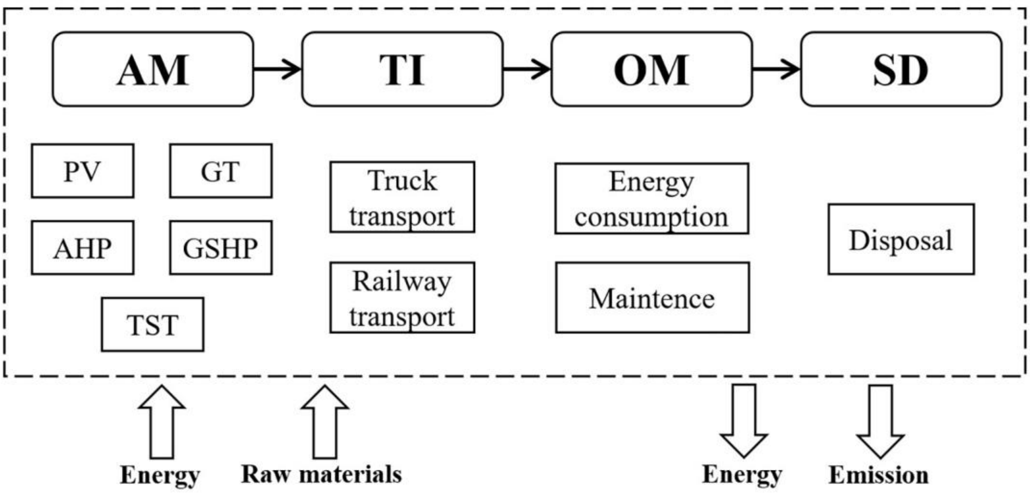

Fig. 3: The system boundary of DES.

Inventory analysis. The data of this part comes from relevant papers, software simulation, investigation, and the database of GaBi. Since a vast amount of data are involved for the assessment of the DES system, it is necessary to simplify the process. When the data's impact on the system results is less than 1% the threshold value, it is considered insignificant to collect these data for the inventory analysis process, thus these data will not be considered. The impact of the data on the system is assessed according to its function unit.

Impact assessment and interpretation. The LCA evaluates the potential environmental impact of the assessed system based on the inventory analysis results. The iterative process of inventory analysis and impact assessment was performed to ensure obtaining a reasonable LCA results. The interpretation is the stage of comprehensive consideration of inventory analysis and impact assessment. The conclusion in the interpretation stage should be consistent with the goal and scope of the study. LCA evaluation results include greenhouse gas emission, terrestrial acidification, marine eutrophication, human carcinogenic toxicity, etc. This paper selects greenhouse gas emissions as the representative evaluation index of environmental impact.

2.4. Entropy-TOPSIS multi-criteria evaluation method

A techno-economic-environment Entropy-TOPSIS multi-criteria evaluation method is proposed for the systematic performance assessment. Entropy is an ideal scale in multi-objective system evaluation and decision-making [48, 49]. The entropy-weighted method determines the weight according to the implicit information contained in the evaluation index results. The lower the information quantity is, the greater the uncertainty will be and the lower the entropy will be. Therefore, in accordance with the characteristics of the entropy value, the importance of indicators can be judged by calculating the size of the entropy value[50]. The procedure for calculating the weights of indicators with the entropy method is shown as follows:

$$\begin{cases} x'_{ij} = \frac{x_{ij} - min(x_j)}{max(x_j) - min(x_j)}, \text{ for } x_{ij} \text{ is positive index} \\ x'_{ij} = \frac{max(x_j) - x_{ij}}{max(x_j) - min(x_j)}, \text{ for } x_{ij} \text{ is negative index} \end{cases} \tag{39}$$

Where x_{ij} represents the *j*-th evaluation index of the *i*-th strategy. The proportion of the *i*-th strategy and *j*-th evaluation index is calculated:

$$P_{ij} = \frac{x'_{ij}}{\sum_{i=1}^{m} x'_{ij}} \tag{40}$$

where m is the number of the operation strategy. The information entropy is calculated according to the index proportion:

$$e_j = -\frac{1}{ln\, m} \sum_{i=1}^{m} P_{ij}\, ln\, P_{ij} \tag{41}$$

Finally, the index weight can be calculated:

$$w_j = \frac{1 - e_j}{\sum_j 1 - e_j} \tag{42}$$

The TOPSIS effectively solves multi-criteria evaluation problems [49, 51]. The basic principle is to rank solutions by calculating the distance of the evaluation objects with the best solution and the distance with the poorest solution. TOPSIS makes the most use of the information of the original data, and its results can accurately reflect the gap between samples[50]. the evaluation index should be normalized:

$$x_{ij,normal} = \frac{x_{ij}}{\sqrt{\sum_{i=1}^{m} x_{ij}^2}} \tag{43}$$

Then the positive and negative ideal solutions can be expressed as:

$$\begin{aligned} X^{+} &= (max\{x_{i1}\}, max\{x_{i2}\}, \ldots, max\{x_{in}\}) \\ X^{-} &= (min\{x_{i1}\}, min\{x_{i2}\}, \ldots, min\{x_{in}\}) \end{aligned} \tag{44}$$

Where X^{+} is the positive ideal solution while X^{-} is the negative ideal solution, and n is the number of the evaluation index which were described in Section 2.3. The Euclidean distance between each operation strategy and the optimal and worst can be calculated as follow:

$$\begin{aligned} D_i^{+} &= \sqrt{\sum_{j=1}^{m} w_j (X_j^{+} - x_{ij})^2} \\ D_i^{-} &= \sqrt{\sum_{j=1}^{m} w_j (X_j^{-} - x_{ij})^2} \end{aligned} \tag{45}$$

The final evaluation results of each operation strategy can be expressed as:

$$CI_i = \frac{D_i^{-}}{D_i^{+} + D_i^{-}} \tag{46}$$

Where CI_i is the evaluation results of the i-th strategy, and the closer it is to 1, the better the strategy's comprehensive performance is.

2.5. Case Study in Wuhan, China

An office building in Wuhan is selected for the case study. The building contains five floors, each floor area is approximately 1000 m^2. The building type, number, and room areas are shown in Table 1.

Table 1: The building room information.

Room type	Numbers	Room area (m^2)
Office	55	39.6
Large conference room	4	79.2
Small conference room	8	39.6
Lounge	4	79.2
Toilet	20	24.8
Corridor (the first floor)	1	237.6
Corridor (the second to fifth floor)	4	198.0
Storehouse	5	39.6

The meteorological data at Wuhan is obtained from the EnergyPlus website. TPL305M-72 PV module is selected and is installed on the building roof with an inclination of 25°. 360 photovoltaic panels are arranged on the building roof; the total capacity of the photovoltaic array is 109.80 kW. The reference efficiency is 15.78%, and the size is 1950*992 mm for each photovoltaic panel. The selected device of the DES under the FTL and FEL is presented in the annex. The device model selection of FELTS is the same as FEL, except that the devices of FELTS have an additional TST with a capacity of 560 kW.

3. Results and discussion

3.1. Energy demand and supply

The energy supply of DES under the FTL for each month in the whole year is presented in Fig 4. For the building's monthly cooling and heating energy supply, AHP is the largest, followed by GSHP and AB. In each month, the amounts of power surplus varies. In April and October, the transitional seasons, the power load is satisfied by the PV system and the grid while the GT is turned off to reduce energy waste. The total power surplus is 4.27×10^5 kWh throughout the year. January has the most significant power surplus, 6.24×10^4 kWh; while October is the month with the least power surplus, 2.06×10^3 kWh. The building energy supply and demand for typical days are shown in the annex.

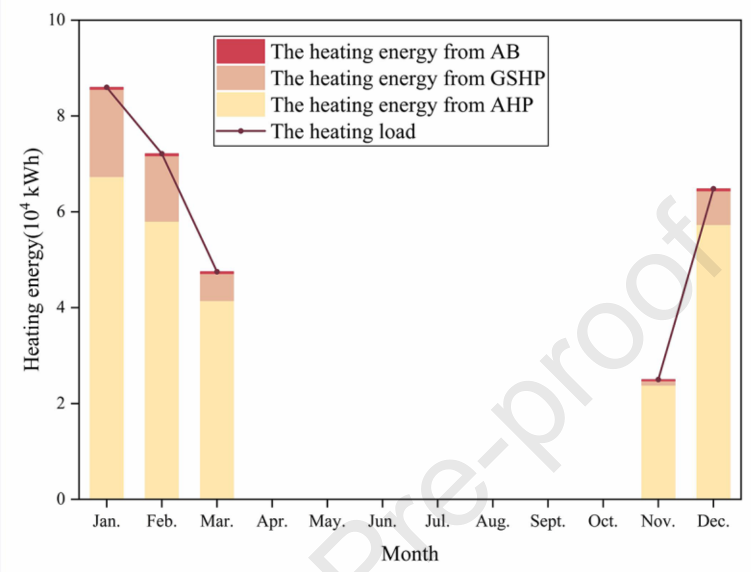

(a)

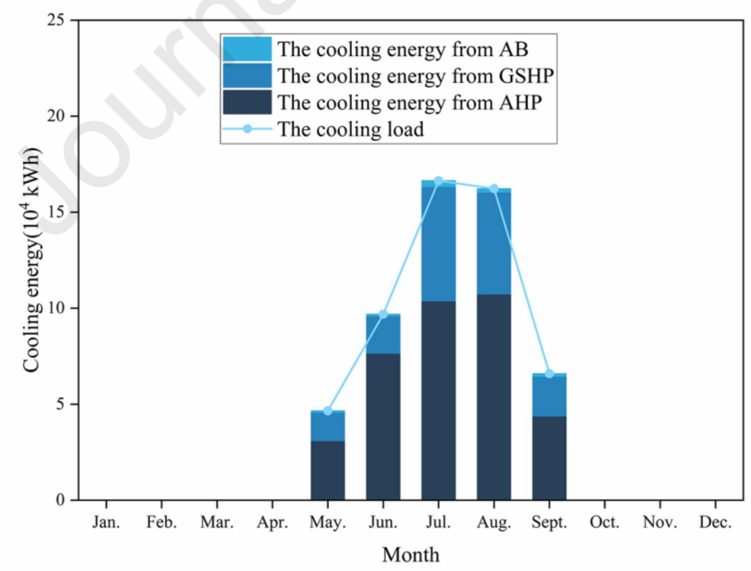

(b)

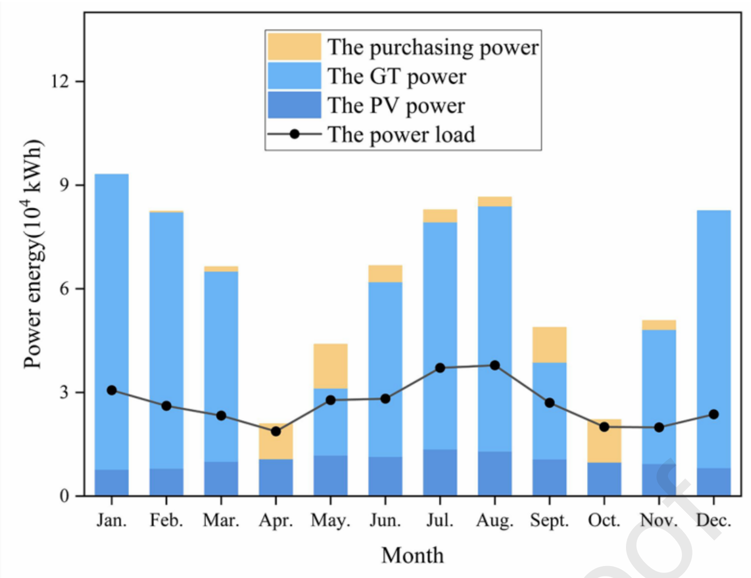

(c)

Fig. 4: Load and energy supply of DES under the FTL (a) Heating (b) Cooling (c) Power.

412 The energy load and supply under the FEL operation strategy are shown in Fig. 5. And there are various cooling and heating surpluses in each month of the year. During the cooling season, August is the month with the largest wasted cooling energy, 8.84×10^4 kWh, while May is the minimum waste cooling energy, 4.99×10^4 kWh. During the heating season, January is the month with the largest wasted heating energy, 5.13×10^4 kWh, while November is the minimum waste heating energy, 2.34×10^4 kWh. The building energy supply and demand for typical days are shown in the annex.

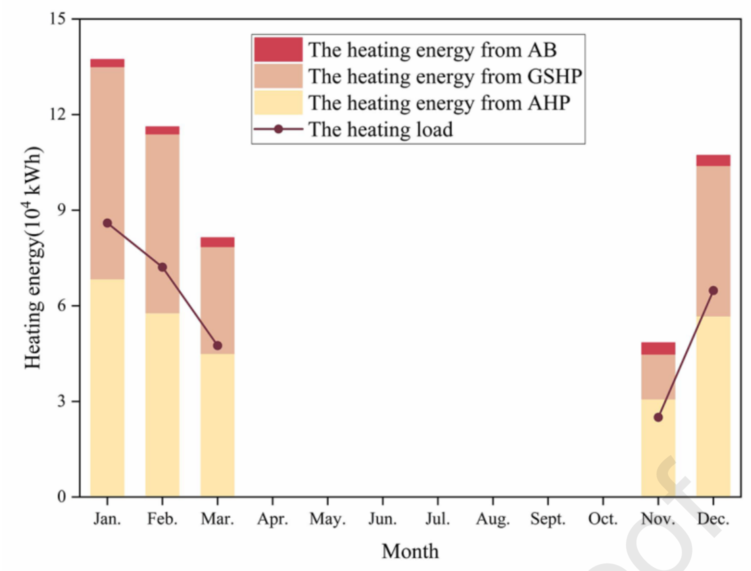
15
12
9
6
3
0
Heating energy(10⁴ kWh)
The heating energy from AB
The heating energy from GSHP
The heating energy from AHP
The heating load
Jan.
Feb.
Mar.
Apr.
May.
Jun.
Jul.
Aug.
Sept.
Oct.
Nov.
Dec.
Month

(a)

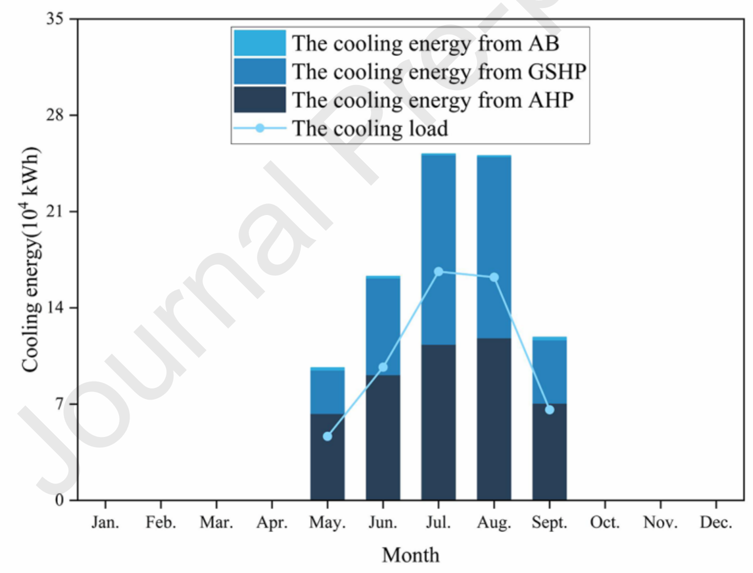
35
28
21
14
7
0
Cooling energy(10⁴ kWh)
The cooling energy from AB
The cooling energy from GSHP
The cooling energy from AHP
The cooling load
Jan.
Feb.
Mar.
Apr.
May.
Jun.
Jul.
Aug.
Sept.
Oct.
Nov.
Dec.
Month

(b)

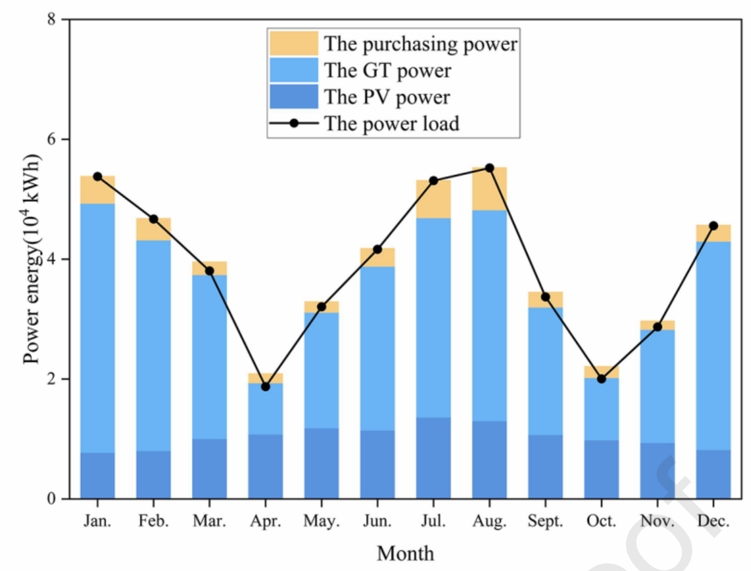

(c)

Fig. 5: Load and energy supply of DES under the FEL (a) Heating (b) Cooling (c) Power.

The energy load and supply under the FELTS are shown in Fig. 6. Compared with the FEL, it dramatically reduces the system's cooling and heating energy surplus each month of the year. During the cooling season, May is the month with a largest wasted cooling energy, 1.43×10^4 kWh, with a proportional reduction of 71.26%. The total yearly wasted cooling and heating energy is 4.89×10^4 kWh, which reduces 90.73% compared with the FEL. Compared with the FEL, the total power consumption stays constant in April and October, while the total power consumption decreased in other months. The yearly power generation of GT and power purchase for FELTS are 2.20×10^5 kWh and 2.95×10^4 kWh respectively and reduced by 29.7% and 22.8% compared with FEL. The building energy supply and demand for typical days are shown in the annex.

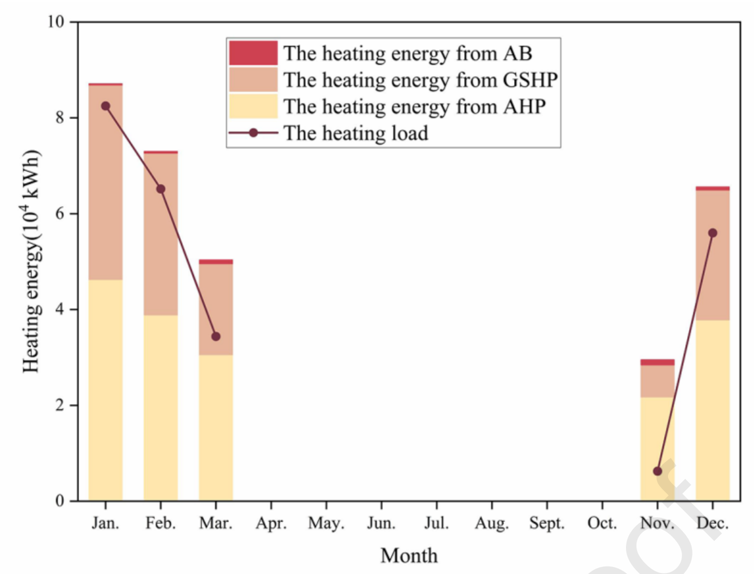

10
8
6
4
2
0
Heating energy(10^4 kWh)
The heating energy from AB
The heating energy from GSHP
The heating energy from AHP
The heating load
Jan.
Feb.
Mar.
Apr.
May.
Jun.
Jul.
Aug.
Sept.
Oct.
Nov.
Dec.
Month

(a)

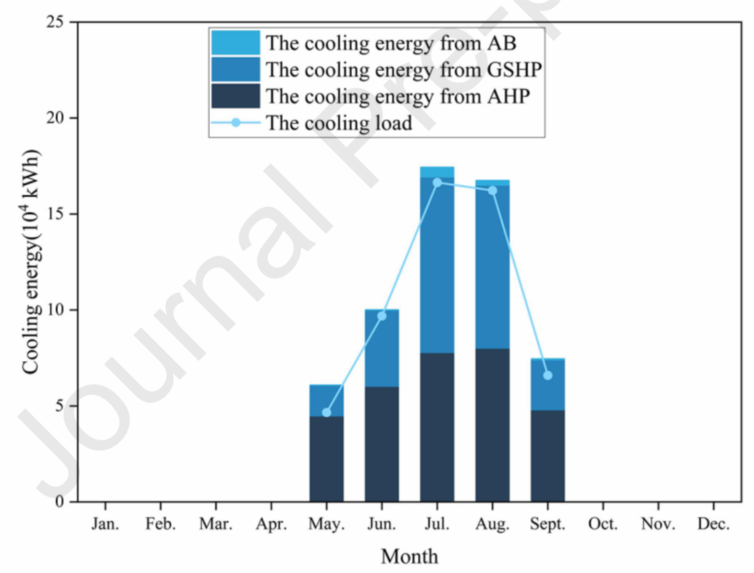

25
20
15
10
5
0
Cooling energy(10^4 kWh)
The cooling energy from AB
The cooling energy from GSHP
The cooling energy from AHP
The cooling load
Jan.
Feb.
Mar.
Apr.
May.
Jun.
Jul.
Aug.
Sept.
Oct.
Nov.
Dec.
Month

(b)

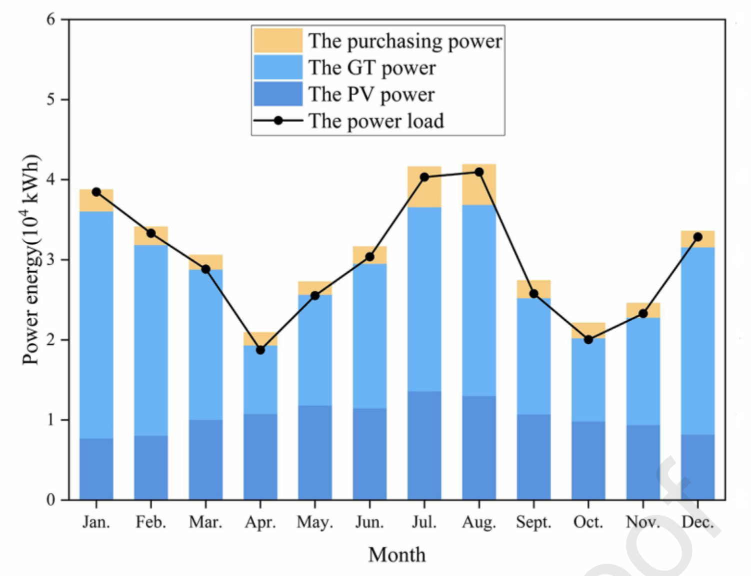

(c)

Fig. 6: Load and energy supply of DES under FELTS (a) Heating (b) Cooling (c) Power.

3.2. Device and Energy Cost

The unit capacity cost for components in the system is shown in Table 2. The price of natural gas is 3.54 CNY/Nm^3, and the time-varying electricity price is shown in Table 3.

Table 2: The unit capacity cost.

Device	Unit	Unit cost
AHP	CNY/kW	1000
GSHP	CNY/kW	1250
PV	CNY/kW	1000
Buried pipe	CNY/m	90
TST	CNY/kW	300
Water pump	CNY/kW	400

Table 3: The sharing price in Wuhan.

Period	Time interval	Price (CNY/kWh)
Peak load	8 p.m. to 10 p.m.	1.2071

High load	9 a.m. to 3 p.m.	1.0070
Ordinary load	7 a.m. to 9 a.m., 3 p.m. to 8 p.m., 10 p.m. to 11 p.m.	0.6907
Low load	11 p.m. to 7 a.m.	0.3550

The cost function of GT is shown as:

$$C_{GT} = \begin{cases} -0.824P_{GT,rated} + 6713.60 (P_{GT} < 4000) \\ -0.168P_{GT,rated} + 4113.92 (P_{GT} \geq 4000) \end{cases} \tag{47}$$

Where C_{GT} is the unit cost of GT, $P_{GT,rated}$ is the nominal capacity of GT.

3.3. DES Performance Analysis

The service life of PV modules, GT, GSHP, and other devices is assumed to be 20 years. Table 4 presents the energy consumption of DES in one life cycle under the three operation strategies.

Table 4: Energy consumption of DES under the three operation strategies.

Item	Unit	FTL	FEL	FELST
Natural gas consumption	Nm^3	3.85×10^6	2.26×10^6	1.54×10^6
Power purchase	kWh	1.21×10^6	7.77×10^5	6.03×10^5
Power generation by GT	kWh	1.12×10^7	6.23×10^6	4.40×10^6
Power generation by PV	kWh	2.50×10^6	2.50×10^6	2.50×10^6
Cooling output by GSHP	kWh	3.35×10^6	8.35×10^6	5.13×10^6
Heating output by GSHP	kWh	9.08×10^5	4.35×10^6	2.56×10^6
Cooling output by AHP (exhaust gas)	kWh	7.25×10^6	9.40×10^6	6.33×10^6
Heating output by AHP (exhaust gas)	kWh	4.96×10^6	6.13×10^6	4.58×10^6
Cooling output by AHP (AB)	kWh	1.57×10^5	1.29×10^5	1.75×10^5
Heating output by AHP (exhaust gas)	kWh	4.02×10^4	2.81×10^5	6.23×10^4
Cooling output by TST	kWh	/	/	3.51×10^6
Heating output by TST	kWh	/	/	2.11×10^6
PEC	kWh	4.13×10^7	2.45×10^7	1.69×10^7
PER	%	51.49	86.78	125.69

The DES is powered by fossil fuel and renewable energy; thus, system efficiency can be improved compared to the traditional centralized energy supply system[53, 54], and various operation strategies lead to different system operating performances. Under the FTL operation strategy, the power generation of GT is 1.12×10^7 kWh, and the cooling and heating output recovering from the exhaust gas are 7.25×10^6 kWh and 4.96×10^6 kWh. The power generation of GT is 6.23×10^6 kWh for FEL, while its cooling and heating output from the exhaust gas are 9.40×10^6 kWh and 6.13×10^6 kWh. It is obvious that the FEL makes more efficient use of waste heat than the FHL; that is, it consumes less non-renewable primary energy with a higher energy utilization efficiency for meeting the building cooling, heating, and power load. In Table 4, the cooling and heating output of GSHP and AHP (exhaust gas) under the FEL are higher than that under the FTL. More generally, the situation is greatly improved with the integration of TST. Compared with the FEL, the system's primary energy input, GT power generation, GSHP output, and AHP (exhaust gas) under the FELTS have a certain amount of reduction. The energy supply of DES is more consistent with the building load under the FELTS, and waste energy is reduced.

The DES system's PEC under the FTL operation strategy is the largest, followed by the FEL and FELTS. The FELTS reduced by 54.8% and 26.7%, respectively, compared with the FTL and FEL. The FELTS has the highest PER among the three operation strategies, 144.1% and 44.8% higher than the FTL and FEL. Notably, the PER of FELTS is higher than 100.0% as the PER of GSHP in the system is more than 100.0%, and the photovoltaic subsystem has an energy output without inputting non-renewable primary energy.

The DES optimization is crucial to system lifecycle cost reduction [7, 24]. According to the model and data, it can be acquired that the economic assessment results of DES under the three operation strategies. The FELTS has the best economic performance, and the economic performance of the DES under the three operation strategies is shown in Table 5. The initial investment of the system for FTL is 3.51×10^6 CNY, and it is slightly larger than that of the other two operation strategies as it has a larger equipment capacity. In terms of the composition of annual operation cost, the natural gas cost accounts for a large proportion while the power purchase cost accounts for a small proportion, which shows that the power demand is mainly satisfied by the DES. In comparison, the annual operation cost of the system under the FTL is the largest, and that of the three strategies are 7.33×10^5 CNY, 4.35×10^5 CNY, and 2.99×10^5 CNY respectively. From the perspective of system DAV, the FTL has the largest DAV, and the DAV of the three operation strategies is 1.05×10^6 CNY, 7.23×10^5 CNY, and 5.94×10^5 CNY.

Table 5: Economic assessment result of DES under three operation strategies (CNY).

Cost categories	FTL	FEL	FELTS
Initial investment	3.51×10^6	3.21×10^6	3.28×10^6
Yearly cost of natural gas	6.81×10^5	4.02×10^5	2.73×10^5
Yearly cost of power	5.20×10^4	3.32×10^4	2.63×10^4
Yearly operation cost	7.33×10^5	4.35×10^5	2.99×10^5
Yearly maintenance cost	9.18×10^3	8.40×10^3	8.57×10^3
DAV	1.05×10^6	7.23×10^5	5.94×10^5

Based on the inventory data of the DES and the calculation results of GaBi software, the corresponding greenhouse gas emissions of the functional unit can be obtained, and the greenhouse gas emissions of the DES at each stage under the three operation strategies are shown in Table 6. The proportions of greenhouse gas emissions of different subsystems under the three operation strategies are shown in Fig. 7. The data of the inventory analysis is shown in the annex.

Table 6: The greenhouse gas emissions of the DES under three operation strategies.

		FTL	FEL	FELTS
PV ($kg\ CO_2eq$)	AM	3.18×10^{-1}	3.18×10^{-1}	3.18×10^{-1}
	TI	1.96×10^{-3}	1.96×10^{-3}	1.96×10^{-3}
	OM	0	0	0
	SD	1.32×10^{-1}	1.32×10^{-1}	1.32×10^{-1}
	Subtotal	4.52×10^{-1}	4.52×10^{-1}	4.52×10^{-1}
GSHP ($kg\ CO_2eq$)	AM	6.28×10^{-1}	7.23×10^{-1}	6.99×10^{-1}
	TI	5.80×10^{-2}	1.02×10^{-1}	8.7810^{-2}
	OM	5.63	6.16	3.19
	SD	1.73×10^{-3}	1.66×10^{-3}	1.61×10^{-3}
	Subtotal	6.32	6.99	3.98
GT (kg CO2eq)	AM	5.65×10^{-2}	2.84×10^{-2}	2.84×10^{-2}
	TI	8.66×10^{-4}	4.33×10^{-4}	4.33×10^{-4}
	OM	22.70	13.30	9.33
	SD	1.03×10^{-4}	5.20×10^{-5}	5.20×10^{-5}
	Subtotal	2.28×10^{1}	1.33×10^{1}	9.36×10^{0}
AHP ($kg\ CO_2eq$)	AM	2.38×10^{-1}	1.86×10^{-1}	1.86×10^{-1}
	TI	1.91×10^{-3}	1.53×10^{-3}	1.53×10^{-3}
	OM	1.03×10^{0}	7.00×10^{-1}	1.75×10^{-1}
	SD	4.25×10^{-4}	3.47×10^{-4}	3.47×10^{-4}
	Subtotal	1.27×10^{0}	8.88×10^{-1}	3.63×10^{-1}
TST ($kg\ CO_2eq$)	AM	0	0	3.72×10^{-2}
	TI	0	0	7.10×10^{-5}
	OM	0	0	0
	SD	0	0	4.40×10^{-5}
	Subtotal	0	0	3.74×10^{-2}
electric equipment ($kg\ CO_2eq$)		5.34	1.14	2.23
Total ($kg\ CO_2eq$)		36.18	22.77	16.40

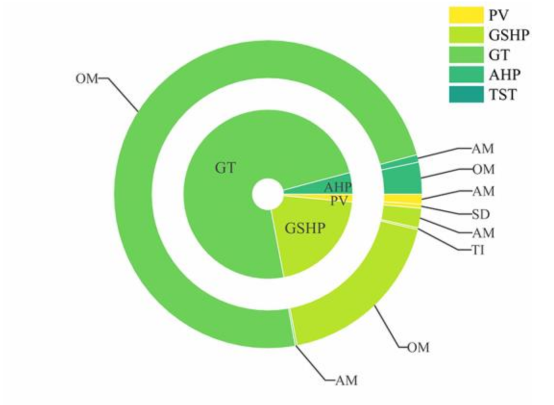

(a) FTL

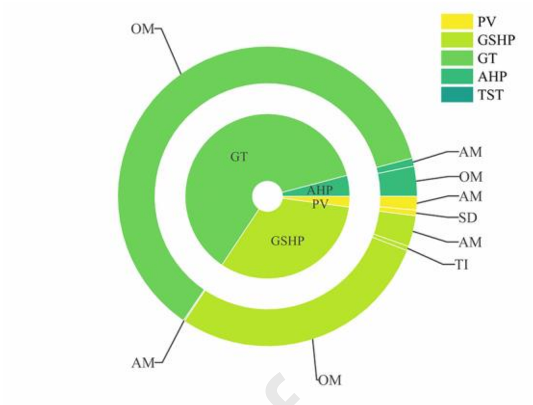

(b) FEL

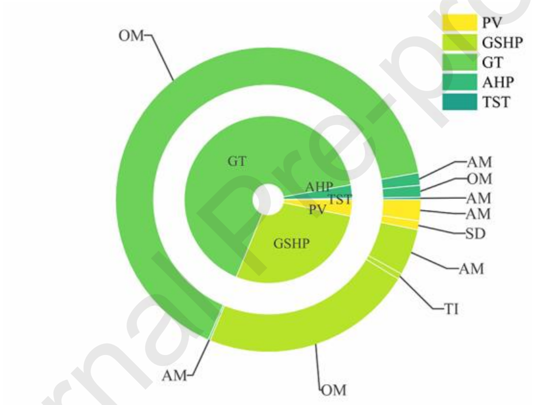

(c) FELTS

Fig. 7: The proportions of greenhouse gas emissions of different subsystems for the three operation strategies.

The LCA provides a comprehensive environmental assessment of energy system equipment and further performance improvements based on the results [55, 56]. From the phased greenhouse gas emissions of each subsystem under the three operation strategies, the greenhouse gas emissions of the PV subsystem are the same, as the capacity of the PV module is the same. Under the FTL and FEL, the greenhouse gas emission at the OM stage accounts for the most significant proportion of the GSHP, GT, and AHP subsystems. In contrast, the greenhouse gas emission in the OM stage of the AHP subsystem is less than that in the AM stage under the FELTS. In terms of greenhouse gas emissions of each subsystem, the GT has the most significant greenhouse gas emissions. Under the three operation strategies, the proportion of GT greenhouse gas emissions in total emissions are 63.0%, 58.3%, and 57.1%, respectively. The greenhouse gas emission of GSHP takes second place, accounting for 17.5%, 30.7%, and 24.3% of the total emissions, respectively. The greenhouse gas emissions of PV are relatively small, highlighting clean energy's advantages.

The GSHP undertakes a significant cooling and heating load under the FEL. At the same time, the environmental performance of the GSHP under FELTS is significantly improved compared with the other two operation strategies. For the GT and AHP subsystems, the FTL has the most significant greenhouse gas emission, which the FEL and FELT follow. The total greenhouse gas emissions for the three operation strategies are 36.2 $kg\ CO_2eq$, 22.8 $kg\ CO_2eq$, and 16.4 $kg\ CO_2eq$ respectively.

Based on the techno-economic-environment assessment, the improvement of DES's environmental performance is from two aspects: first is to maximize building demand-supply fit by selecting the appropriate equipment model and configuration, and second is to use clean and renewable energy such as solar energy.

The comprehensive system evaluation is based on the technology, economy, and environment, and the entropy-TOPSIS method is employed as previously described. This paper selects two indicators to evaluate the system's performance in technology, PER, and the degree of dependence on foreign energy (DFE). The DFE consists of the power purchase cost and gas purchase cost. The economic evaluation includes DAV and initial investment (II), while the greenhouse gas emission (GGE) is the environmental evaluation index. The five evaluation indexes of DES under three operation strategies are shown in Table 7.

Table 7: The five evaluation indexes of DES under three operation strategies.

Index	FTL	FEL	FELTS
PER	51.49%	86.78%	125.69%
DFE	7.33×10^5 CNY	4.35×10^5 CNY	2.99×10^5 CNY
DAV	1.05×10^6 CNY	7.23×10^5 CNY	5.94×10^5 CNY
II	3.51×10^6 CNY	3.21×10^6 CNY	3.28×10^6 CNY
GGE	36.18 $kg\ CO_2eq$	22.77 $kg\ CO_2eq$	16.42 $kg\ CO_2eq$

The above five original evaluation index data determine each index's weight by the entropy weight method, as shown in Table 8. The indexes under different operation strategies are normalized firstly, and the results are shown in Fig. 8. Fig. 8 indicates that the FELTS has the best performance in PER, DFE, DAV, and GGE. The FEL has the best performance in II as the system of the FELTS is more complex. Meanwhile, it also shows that the FELTS is consistent with the optimal result except for the performance of II.

Table 8: The weight of evaluation indicators.

Index	PER	DFE	DAV	II	GGE
Weight (%)	21.86	19.67	19.49	19.27	19.92

The energy efficiency in the building sector can be improved by energy management, and the system design and operation strategies are optimized to achieve energy savings and emission reductions [57]. The comprehensive evaluation method of the building energy supply system is also a research highlight [33]. The Entropy-TOPSIS method integrates the technical, economic, and environmental assessment for building-distributed energy systems and allows for further improvements to be made to the optimal solution. The comprehensive performance of DES under three operation strategies is evaluated by the Entropy-TOPSIS method, and the evaluation results of the three operation strategies are 0, 0.49, and 0.99, respectively. Compared with the other two operation strategies, the system comprehensive performance under the FELTS is optimal from technical and environmental evaluation aspects. The final evaluation result of Entropy-TOPSIS method indicates that the FELTS has the best performance as its evaluation result is close to 1.

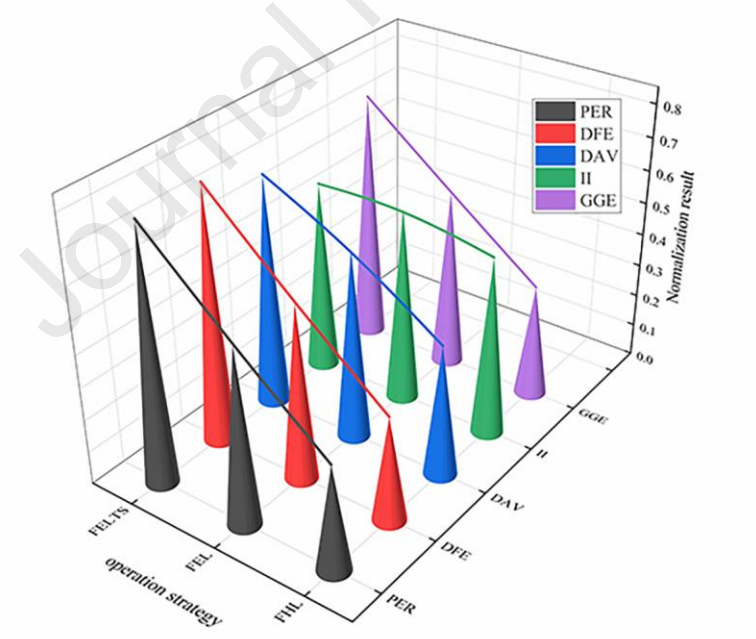

Fig. 8: Normalized results of the evaluation index for the three operation strategies.

4. Conclusion

This study presents the modeling and techno-economic-environment assessment of a building-distributed energy system consisting of the PV, GSHP, GT, AHP, and TST. The system design and operation performance are established and evaluated under three control strategies - the FTL, FEL, and FELTS. An office building in Wuhan, China, was selected for the case study. Some conclusions are summarized as follows.

The result showed that the technological evaluation index PER of DES under FTL, FEL, and FELTS are 51.49%, 86.78%, and 125.69%, respectively. The building demand-supply fit is significantly improved under the FELTS strategy. Under the FTL and FEL operation strategy, there was much-wasted power and thermal energy. The economic evaluation index DAV of the system under FTL, FEL, and FELTS is 1.05×10^6 CNY, 7.23×10^5 CNY, and 5.94×10^5 CNY, respectively. Operating under the FELTS is the most economical. Environment evaluation results showed that the GT subsystem has the largest greenhouse gas emissions in the DES under the three operation strategies, GSHP subsystem contributes to the second-largest emissions. The total greenhouse gas emissions of the three operation strategies are 36.2 kg CO_2eq, 22.8 kg CO_2eq, and 16.4 kg CO_2eq, respectively. The Entropy-TOPSIS results showed that the comprehensive performance of the DES under the FELTS is the best, followed by the FEL and FTL.

This research work proposes simulation and comprehensive evaluation methods for DES, and it provides the theoretical basis for multi-objective optimization and energy management of DES. This preliminary research work will promote the development and application of decentralized energy production and supply for decarbonization in the building section while meeting increasing energy demand. Future work will investigate the grid's and DES's interactive correlation to achieve optimized techno-economic-environmental performance; energy or carbon trading scenarios could be considered. The resilience of the distributed energy system under interrupted conditions (extreme weather, cyber attack, etc.) can be also investigated.

Funding

This work was supported by National Natural Science Foundation of China (No. 52076099), the Graduates' Innovation Fund, Huazhong University of Science and Technology (No. 2020yjsCXCY067) and the Open Research Project Program of the State Key Laboratory of Internet of Things for Smart City (University of Macau) (No. SKL-IoTSC(UM)-2021-2023/ORPF/SA13/2022). We also would like to thank members of the Harvard-China Project on Energy, Economy and Environment for useful comments and suggestions, and the Harvard Global Institute for an award to the Harvard-China Project on Energy, Economy and Environment.

References

[1] X. Li, W. Wu, and C. W. F. Yu, "Energy demand for hot water supply for indoor environments: Problems and perspectives," *Indoor and Built Environment,* vol. 24, no. 1, pp. 5-10, 2015/02/01 2014, doi: 10.1177/1420326X14564285.

[2] S. Guo, D. Yan, S. Hu, and Y. Zhang, "Modelling building energy consumption in China under different future scenarios," *Energy,* vol. 214, p. 119063, 2021/01/01/ 2021, doi: https://doi.org/10.1016/j.energy.2020.119063.

[3] H. Cho, A. D. Smith, and P. Mago, "Combined cooling, heating and power: A review of performance improvement and optimization," *Applied Energy,* vol. 136, pp. 168-185, 2014/12/31/ 2014, doi: https://doi.org/10.1016/j.apenergy.2014.08.107.

[4] J. Yan, O. A. Broesicke, X. Tong, D. Wang, D. Li, and J. C. Crittenden, "Multidisciplinary design optimization of distributed energy generation systems: The trade-offs between life cycle environmental and economic impacts," *Applied Energy,* vol. 284, p. 116197, 2021/02/15/ 2021, doi:

https://doi.org/10.1016/j.apenergy.2020.116197.

[5] S. Thiangchanta, T. A. Do, P. Suttakul, and Y. Mona, "Energy reduction of split-type air conditioners using a pre-cooling system for the condenser," *Energy Reports,* vol. 7, pp. 1-6, 2021/09/01/ 2021, doi: https://doi.org/10.1016/j.egyr.2021.05.055.

[6] A. A. Saari, "Distributed energy generation and sustainable development," *Renewable and Sustainable Energy Reviews,* 2006.

[7] W. Ma, S. Fang, and G. Liu, "Hybrid optimization method and seasonal operation strategy for distributed energy system integrating CCHP, photovoltaic and ground source heat pump," *Energy,* vol. 141, pp. 1439-1455, 2017/12/15/ 2017, doi: https://doi.org/10.1016/j.energy.2017.11.081.

[8] J. Hou, J. Wang, Y. Zhou, and X. Lu, "Distributed energy systems: Multi-objective optimization and evaluation under different operational strategies," *Journal of Cleaner Production,* vol. 280, p. 124050, 2021/01/20/ 2021, doi: https://doi.org/10.1016/j.jclepro.2020.124050.

[9] T. Guan, H. Lin, Q. Sun, and R. Wennersten, "Optimal configuration and operation of multi-energy complementary distributed energy systems," *Energy Procedia,* vol. 152, pp. 77-82, 2018/10/01/ 2018, doi: https://doi.org/10.1016/j.egypro.2018.09.062.

[10] Al *et al.*, "Review of tri-generation technologies: Design evaluation, optimization, decision-making, and selection approach," *Energy Conversion & Management,* 2016.

[11] D. W. Wu and R. Z. Wang, "Combined cooling, heating and power: A review," *Progress in Energy and Combustion Science,* vol. 32, no. 5–6, pp. 459-495, 2006.

[12] J. Wang, Z. Han, and Z. Guan, "Hybrid solar-assisted combined cooling, heating, and power systems: A review - ScienceDirect," *Renewable and Sustainable Energy Reviews,* vol. 133.

[13] F. Cheng *et al.*, "Novel Quasi-Solid-State Electrolytes based on Electrospun Poly(vinylidene fluoride) Fiber Membranes for Highly Efficient and Stable Dye-Sensitized Solar Cells," (in eng), *Nanomaterials (Basel),* vol. 9, no. 5, p. 783, 2019, doi: 10.3390/nano9050783.

[14] G. Yang and X. Q. Zhai, "Optimal design and performance analysis of solar hybrid CCHP system considering influence of building type and climate condition," *Energy,* vol. 174, pp. 647-663, 2019/05/01/ 2019, doi: https://doi.org/10.1016/j.energy.2019.03.001.

[15] E. Cardona, A. Piacentino, and F. Cardona, "Matching economical, energetic and environmental benefits: An analysis for hybrid CHCP-heat pump systems," *Energy Conversion and Management,* vol. 47, no. 20, pp. 3530-3542, 2006/12/01/ 2006, doi: https://doi.org/10.1016/j.enconman.2006.02.027.

[16] R. Zeng, X. Zhang, Y. Deng, H. Li, and G. Zhang, "Optimization and performance comparison of combined cooling, heating and power/ground

source heat pump/photovoltaic/solar thermal system under different load ratio for two operation strategies," *Energy Conversion and Management,* vol. 208, p. 112579, 2020/03/15/ 2020, doi: https://doi.org/10.1016/j.enconman.2020.112579.

[17] B. Chen and Y. E. Caihua, "Application of Combined Cooling,Heating and Power System Coupled with Groundsource Heat Pump," *Gas & Heat,* 2014.

[18] F. A. Boyaghchi, M. Chavoshi, and V. Sabeti, "Optimization of a novel combined cooling, heating and power cycle driven by geothermal and solar energies using the water/CuO (copper oxide) nanofluid," *Energy,* vol. 91, pp. 685-699, 2015/11/01/ 2015, doi: https://doi.org/10.1016/j.energy.2015.08.082.

[19] W. Lombardo, A. Sapienza, S. Ottaviano, L. Branchini, A. De Pascale, and S. Vasta, "A CCHP system based on ORC cogenerator and adsorption chiller experimental prototypes: Energy and economic analysis for NZEB applications," *Applied Thermal Engineering,* vol. 183, p. 116119, 2021/01/25/ 2021, doi: https://doi.org/10.1016/j.applthermaleng.2020.116119.

[20] J. Wang, C. Ma, and J. Wu, "Thermodynamic analysis of a combined cooling, heating and power system based on solar thermal biomass gasification☆," *Applied Energy,* vol. 247, pp. 102-115, 2019/08/01/ 2019, doi: https://doi.org/10.1016/j.apenergy.2019.04.039.

[21] M. Mehrpooya, M. Sadeghzadeh, A. Rahimi, and M. Pouriman, "Technical performance analysis of a combined cooling heating and power (CCHP) system based on solid oxide fuel cell (SOFC) technology – A building application," *Energy Conversion and Management,* vol. 198, p. 111767, 2019/10/15/ 2019, doi: https://doi.org/10.1016/j.enconman.2019.06.078.

[22] J. Zhang, S. Cao, L. Yu, and Y. Zhou, "Comparison of combined cooling, heating and power (CCHP) systems with different cooling modes based on energetic, environmental and economic criteria," *Energy Conversion and Management,* vol. 160, pp. 60-73, 2018/03/15/ 2018, doi: https://doi.org/10.1016/j.enconman.2018.01.019.

[23] H. Ren, Y. Lu, Y. Zhang, F. Chen, and X. Yang, "Operation Simulation and Optimization of Distributed Energy System Based on TRNSYS," *Energy Procedia,* vol. 152, pp. 3-8, 2018/10/01/ 2018, doi: https://doi.org/10.1016/j.egypro.2018.09.050.

[24] X. Zhu *et al.*, "The optimal design and operation strategy of renewable energy-CCHP coupled system applied in five building objects," *Renewable Energy,* vol. 146, pp. 2700-2715, 2020/02/01/ 2020, doi: https://doi.org/10.1016/j.renene.2019.07.011.

[25] F. Ren, J. Wang, S. Zhu, and Y. Chen, "Multi-objective optimization of combined cooling, heating and power system integrated with solar and geothermal energies," *Energy Conversion and Management,* vol. 197, p. 111866, 2019/10/01/ 2019, doi: https://doi.org/10.1016/j.enconman.2019.111866.

[26] B. K. Das, Y. M. Al-Abdeli, and G. Kothapalli, "Effect of load following strategies, hardware, and thermal load distribution on stand-alone hybrid CCHP systems," *Applied Energy,* vol. 220, pp. 735-753, 2018/06/15/ 2018, doi: https://doi.org/10.1016/j.apenergy.2018.03.068.

[27] C. Brandoni, M. Renzi, F. Caresana, and F. Polonara, "Simulation of hybrid renewable microgeneration systems for variable electricity prices," *Applied Thermal Engineering,* vol. 71, no. 2, pp. 667-676, 2014/10/22/ 2014, doi: https://doi.org/10.1016/j.applthermaleng.2013.10.044.

[28] M. Li, X. Z. Jiang, D. Zheng, G. Zeng, and L. Shi, "Thermodynamic boundaries of energy saving in conventional CCHP (Combined Cooling, Heating and Power) systems," *Energy,* vol. 94, pp. 243-249, 2016/01/01/ 2016, doi: https://doi.org/10.1016/j.energy.2015.11.005.

[29] K. Yang, N. Zhu, and T. Yuan, "Analysis of optimum scale of biomass gasification combined cooling heating and power (CCHP) system based on life cycle assessment(LCA)," *Procedia Engineering,* vol. 205, pp. 145-152, 2017/01/01/ 2017, doi: https://doi.org/10.1016/j.proeng.2017.09.946.

[30] Y.-Y. Jing, H. Bai, J.-J. Wang, and L. Liu, "Life cycle assessment of a solar combined cooling heating and power system in different operation strategies," *Applied Energy,* vol. 92, pp. 843-853, 2012/04/01/ 2012, doi: https://doi.org/10.1016/j.apenergy.2011.08.046.

[31] A. Peppas, K. Kollias, A. Politis, L. Karalis, M. Taxiarchou, and I. Paspaliaris, "Performance evaluation and life cycle analysis of RES-hydrogen hybrid energy system for office building," *International Journal of Hydrogen Energy,* vol. 46, no. 9, pp. 6286-6298, 2021/02/03/ 2021, doi: https://doi.org/10.1016/j.ijhydene.2020.11.173.

[32] C. Y. Li, J. Y. Wu, Y. J. Dai, and C.-H. Wang, "Multi-criteria optimization of a biomass gasification-based combined cooling, heating, and power system integrated with an organic Rankine cycle in different climate zones in China," *Energy Conversion and Management,* vol. 243, p. 114364, 2021/09/01/ 2021, doi: https://doi.org/10.1016/j.enconman.2021.114364.

[33] E. Wang, N. Alp, J. Shi, C. Wang, X. Zhang, and H. Chen, "Multi-criteria building energy performance benchmarking through variable clustering based compromise TOPSIS with objective entropy weighting," *Energy,* vol. 125, pp. 197-210, 2017/04/15/ 2017, doi: https://doi.org/10.1016/j.energy.2017.02.131.

[34] D. Wang *et al.*, "A method for evaluating both shading and power generation effects of rooftop solar PV panels for different climate zones of China," *Solar Energy,* vol. 205, pp. 432-445, 2020/07/15/ 2020, doi: https://doi.org/10.1016/j.solener.2020.05.009.

[35] Z. Pan, N. V. Quynh, Z. M. Ali, S. Dadfar, and T. Kashiwagi, "Enhancement of maximum power point tracking technique based on PV-Battery system using hybrid BAT algorithm and fuzzy controller," *Journal of Cleaner Production,* vol. 274, p. 123719, 2020/11/20/ 2020, doi:

https://doi.org/10.1016/j.jclepro.2020.123719.

[36] A. E. Mazraeh, M. Babayan, M. Yari, A. M. Sefidan, and S. C. Saha, "Theoretical study on the performance of a solar still system integrated with PCM-PV module for sustainable water and power generation," *Desalination,* vol. 443, pp. 184-197, 2018/10/01/ 2018, doi: https://doi.org/10.1016/j.desal.2018.05.024.

[37] S. Wu, Y. Dai, X. Li, F. Oppong, and C. Xu, "A review of ground-source heat pump systems with heat pipes for energy efficiency in buildings," *Energy Procedia,* vol. 152, pp. 413-418, 2018/10/01/ 2018, doi: https://doi.org/10.1016/j.egypro.2018.09.167.

[38] A. Girard, E. J. Gago, T. Muneer, and G. Caceres, "Higher ground source heat pump COP in a residential building through the use of solar thermal collectors," *Renewable Energy,* vol. 80, pp. 26-39, 2015/08/01/ 2015, doi: https://doi.org/10.1016/j.renene.2015.01.063.

[39] J. M. Gordon, K. C. Ng, and H. T. Chua, "Centrifugal chillers: Thermodynamic modelling and a diagnostic case study," *International Journal of Refrigeration,* vol. 18, no. 4, pp. 253-257, 1995/05/01/ 1995, doi: https://doi.org/10.1016/0140-7007(95)96863-2.

[40] Z. F. Huang, Y. D. Wan, K. Y. Soh, and K. J. Chua, "Hybrid operating method to improve the part-load performance of gas turbine based combined cooling and power system," *Energy Conversion and Management,* vol. 226, p. 113506, 2020/12/15/ 2020, doi: https://doi.org/10.1016/j.enconman.2020.113506.

[41] E. Mohammadi and M. Montazeri-Gh, "A fuzzy-based gas turbine fault detection and identification system for full and part-load performance deterioration," *Aerospace Science and Technology,* vol. 46, pp. 82-93, 2015/10/01/ 2015, doi: https://doi.org/10.1016/j.ast.2015.07.002.

[42] A. Costantino, S. Calvet, and E. Fabrizio, "Identification of energy-efficient solutions for broiler house envelopes through a primary energy approach," *Journal of Cleaner Production,* vol. 312, p. 127639, 2021/08/20/ 2021, doi: https://doi.org/10.1016/j.jclepro.2021.127639.

[43] A. Shafieian and M. Khiadani, "Integration of heat pipe solar water heating systems with different residential households: An energy, environmental, and economic evaluation," *Case Studies in Thermal Engineering,* vol. 21, p. 100662, 2020/10/01/ 2020, doi: https://doi.org/10.1016/j.csite.2020.100662.

[44] Z. Sadeghi, H. R. Horry, and S. Khazaee, "An economic evaluation of Iranian natural gas export to Europe through proposed pipelines," *Energy Strategy Reviews,* vol. 18, pp. 1-17, 2017/12/01/ 2017, doi: https://doi.org/10.1016/j.esr.2017.09.013.

[45] T. Ghosh and B. R. Bakshi, "Designing hybrid life cycle assessment models based on uncertainty and complexity," *The International Journal of Life Cycle Assessment,* vol. 25, no. 11, pp. 2290-2308, 2020/11/01 2020, doi: 10.1007/s11367-020-01826-5.

[46] X. Yang, S. Zhang, and K. Wang, "Quantitative study of life cycle carbon emissions from 7 timber buildings in China," *The International Journal of Life Cycle Assessment,* vol. 26, no. 9, pp. 1721-1734, 2021/09/01 2021, doi: 10.1007/s11367-021-01960-8.

[47] G. Luderer *et al.*, "Environmental co-benefits and adverse side-effects of alternative power sector decarbonization strategies," *Nature Communications*.

[48] H. Xu, C. Ma, J. Lian, K. Xu, and E. Chaima, "Urban flooding risk assessment based on an integrated k-means cluster algorithm and improved entropy weight method in the region of Haikou, China," *Journal of Hydrology,* vol. 563, pp. 975-986, 2018/08/01/ 2018, doi: https://doi.org/10.1016/j.jhydrol.2018.06.060.

[49] W. Huang, B. Shuai, Y. Sun, Y. Wang, and E. Antwi, "Using entropy-TOPSIS method to evaluate urban rail transit system operation performance: The China case," *Transportation Research Part A: Policy and Practice,* vol. 111, pp. 292-303, 2018/05/01/ 2018, doi: https://doi.org/10.1016/j.tra.2018.03.025.

[50] Y. Zhang, Y. Zhang, H. Zhang, and Y. Zhang, "Evaluation on new first-tier smart cities in China based on entropy method and TOPSIS," *Ecological Indicators,* vol. 145, p. 109616, 2022/12/01/ 2022, doi: https://doi.org/10.1016/j.ecolind.2022.109616.

[51] J. M. Sánchez-Lozano, M. S. García-Cascales, and M. T. Lamata, "Comparative TOPSIS-ELECTRE TRI methods for optimal sites for photovoltaic solar farms. Case study in Spain," *Journal of Cleaner Production,* vol. 127, pp. 387-398, 2016/07/20/ 2016, doi: https://doi.org/10.1016/j.jclepro.2016.04.005.

[52] A. Hss, B. Hjs, and C. Esl, "An extension of TOPSIS for group decision making - ScienceDirect," *Mathematical and Computer Modelling,* vol. 45, no. 7–8, pp. 801-813, 2007.

[53] M. Bilardo, M. Ferrara, and E. Fabrizio, "Performance assessment and optimization of a solar cooling system to satisfy renewable energy ratio (RER) requirements in multi-family buildings," *Renewable Energy,* vol. 155, pp. 990-1008, 2020/08/01/ 2020, doi: https://doi.org/10.1016/j.renene.2020.03.044.

[54] C. Mokhtara, B. Negrou, N. Settou, B. Settou, and M. M. Samy, "Design optimization of off-grid Hybrid Renewable Energy Systems considering the effects of building energy performance and climate change: Case study of Algeria," *Energy,* vol. 219, p. 119605, 2021/03/15/ 2021, doi: https://doi.org/10.1016/j.energy.2020.119605.

[55] A. S. Marques, M. Carvalho, A. A. V. Ochoa, R. Abrahão, and C. A. C. Santos, "Life cycle assessment and comparative exergoenvironmental evaluation of a micro-trigeneration system," *Energy,* vol. 216, p. 119310, 2021/02/01/ 2021, doi: https://doi.org/10.1016/j.energy.2020.119310.

[56] C. Y. Li, J. Y. Wu, C. Chavasint, S. Sampattagul, T. Kiatsiriroat, and R. Z. Wang, "Multi-criteria optimization for a biomass gasification-integrated combined cooling, heating, and power system based on life-cycle assessment," *Energy Conversion and Management,* vol. 178, pp. 383-399, 2018/12/15/ 2018, doi:

https://doi.org/10.1016/j.enconman.2018.10.043.

[57] D. Mariano-Hernández, L. Hernández-Callejo, A. Zorita-Lamadrid, O. Duque-Pérez, and F. Santos García, "A review of strategies for building energy management system: Model predictive control, demand side management, optimization, and fault detect & diagnosis," *Journal of Building Engineering,* vol. 33, p. 101692, 2021/01/01/ 2021, doi: https://doi.org/10.1016/j.jobe.2020.101692.

Declaration of interests

☒ The authors declare that they have no known competing financial interests or personal relationships that could have appeared to influence the work reported in this paper.

☐The authors declare the following financial interests/personal relationships which may be considered as potential competing interests: